

Distribution and biological properties of oceanic water masses around the South Island, New Zealand

W. F. VINCENT*

C. HOWARD-WILLIAMS

Taupo Research Laboratory
DSIR Marine and Freshwater
Department of Scientific and Industrial Research
P. O. Box 415, Taupo, New Zealand

*Present address: Département de biologie, Université
Laval, Québec G1K 7P4, Canada

P. TILDESLEY

E. BUTLER

CSIRO Marine Laboratories
P. O. Box 1538, Hobart, Tasmania, Australia

Abstract The distribution of phytoplankton and the diversity of environmental conditions for their growth around the South Island, New Zealand, were examined in May 1989 by way of chlorophyll *a* fluorescence profiling in combination with discrete sample analysis of nutrients and particulates, CTD-profiles, and concurrent satellite images of sea surface temperature (SST). A composite of 7 overlaid SST images from the period of the cruise emphasised the strong north–south and east–west gradients in the oceanic environment. Water column sampling coupled with SST imagery was used to examine the frontal structure in Cook Strait, upwelling along the West Coast, gradients across the Solander Trough and through Foveaux Strait, and oceanographic features associated with the Subtropical Convergence off the East Coast and over Chatham Rise. A correlation analysis of the near-surface water properties showed the zonal relationships between nutrients, nutrient ratios, and temperature, but also underscored the strong local influence of freshwater inputs around the South Island coastline. An analysis of the *in vivo* fluorescence data revealed large site-to-site differences

in the fluorescence yield per unit extracted chlorophyll *a*. The yield varied systematically with changes in the physical and biological environment across the Subtropical Convergence.

Keywords Chatham Rise; chlorophyll *a*; Cook Strait; fiords; Foveaux Strait; Mernoo Bank; New Zealand; nutrients; phytoplankton; salinity; South Island; Subtropical Convergence; temperature; upwelling

INTRODUCTION

The South Island of New Zealand has a major influence on the physical and chemical properties of the ocean which surrounds it, and these properties are in turn likely to have a controlling effect on biological processes. The coastal waters of this region contain areas of strong boundary forcing, wind-induced upwelling, sharp gradients in mixed-layer depth induced by river inflows, fronts, gyres, plumes, and many other features (see Heath 1985) likely to create a diverse range of biological conditions. Additionally, the South Island lies adjacent to a circumglobal front, the Subtropical Convergence (STC). This major front separates subtropical water in the north from subantarctic water to the south (Heath 1976; Stanton & Ridgway 1988) and is accompanied by strong physical and nutrient gradients which have major implications for planktonic growth.

The dynamic nature of these complex oceanographic features through time and space usually makes it very difficult to interpret biological data collected from discrete locations. However, the concurrent application of physical and biological profiling in the ocean with real-time satellite imagery provides a powerful combination to define adequately the vertical and horizontal structure of the plankton and its environment. This approach has not been used before in New Zealand, but relatively clear skies in May 1989 allowed for a good set of satellite images of sea surface temperature during a cruise designed to describe the oceanographic diversity around the South Island.

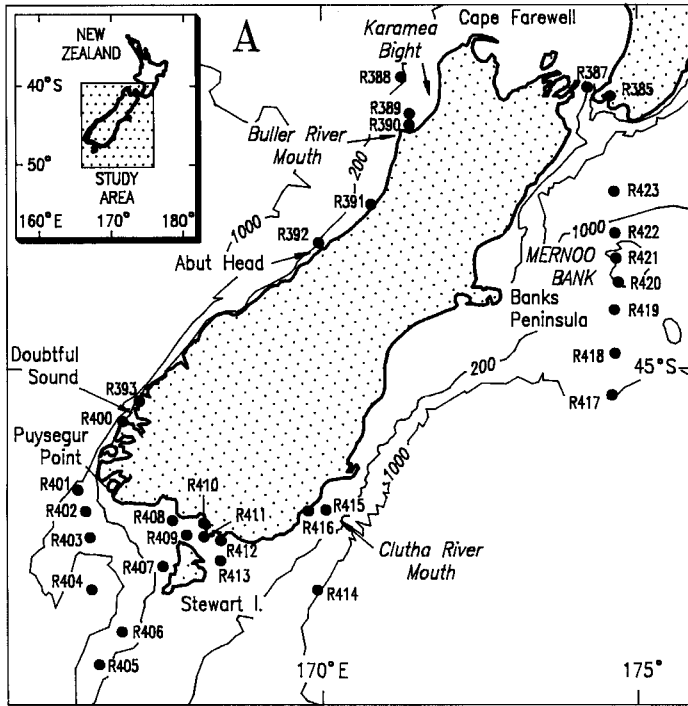
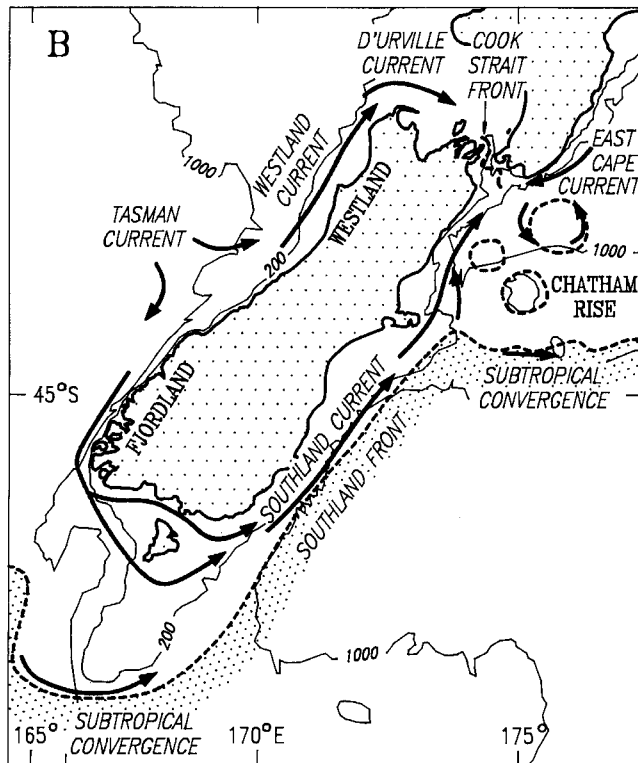


Fig. 1 Map of the South Island, New Zealand. A, Stations for RV *Rapuhia* Cruise 2027. B, The major fronts and currents around the South Island derived from Heath (1985), Barnes (1985), and Bowman et al. (1983) in combination with data from the present cruise.



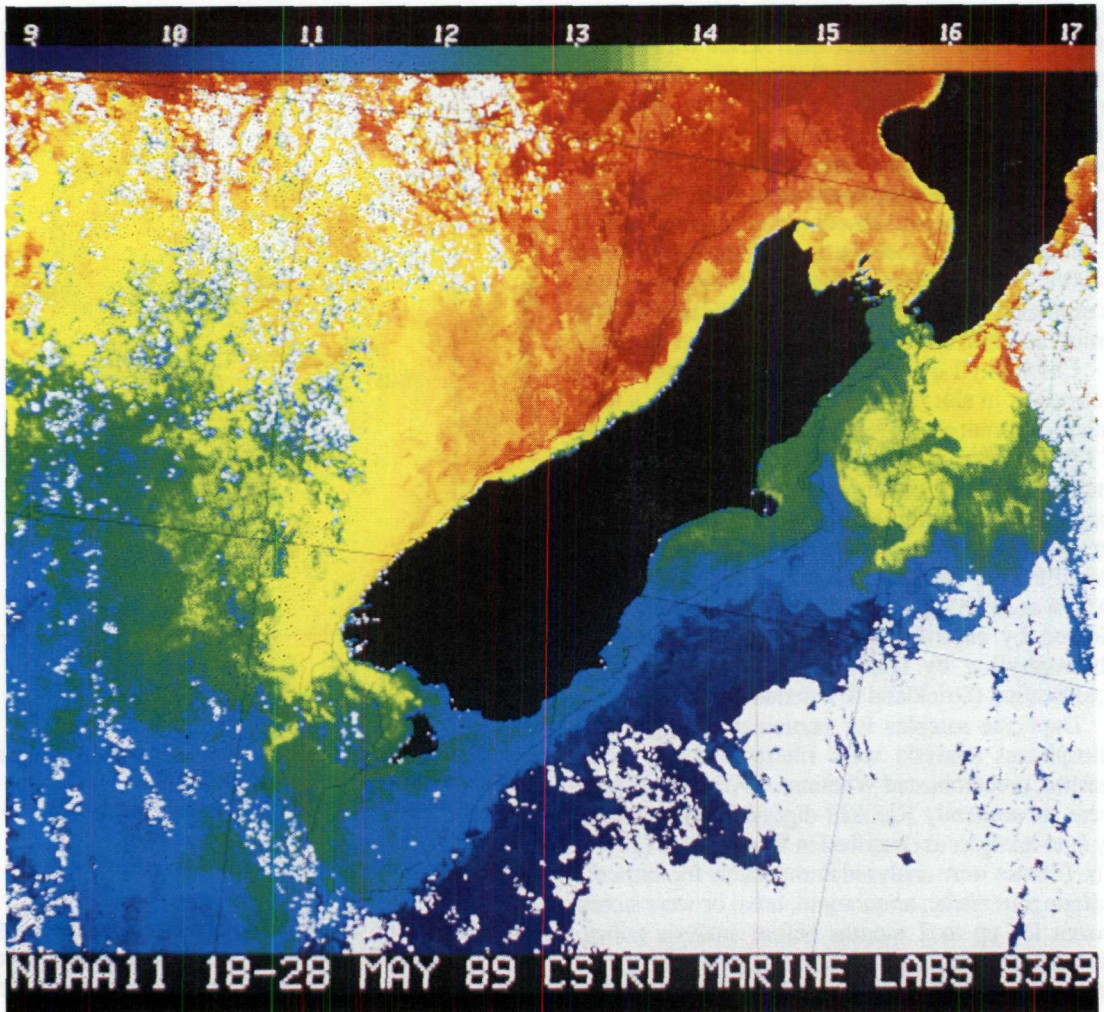


Fig. 2 Composite of seven SST images over the South Island region for the period 18–28 May 1989. The 200 m isobath is marked in this and subsequent images.

In this paper we first examine the general distribution of water masses around the South Island by way of satellite imagery and CTD profiling. We then focus on the water column properties and horizontal gradients at several key locations: the Cook Strait front, the West Coast upwelling region, the Puysegur Bank–Solander Trough area at the southwestern corner of the South Island, Foveaux Strait, and the Subtropical Convergence across the Chatham Rise. Finally, using the pooled data from this diverse range of oceanic environments, we explore the relative relationships between physical, chemical, and biological variables.

METHODS

All profiling was conducted during Cruise 2027 of RV *Rapuhia* between 16 and 29 May 1989. The cruise track encircled the South Island (Fig. 1A) and included 7 stations off the west coast, 5 south-west of the South Island, 6 through Foveaux Strait (between the South Island and Stewart Island), and 7 across the Chatham Rise on the eastern side of the island, as well as additional stations to sample specific oceanographic features.

For conductivity and temperature profiling, a Guildline Model 8755 Conductivity-Temperature-Depth instrument was used mounted on a rosette

sampler. The thermistor was calibrated immediately after the cruise in a water bath series with a PRT bridge, Automatic Systems Laboratories Model F6, which was calibrated to the triple point of water. Samples for conductivity-salinity calibration were taken during the cruise from regions of the water column with stable temperature and salinity properties. These samples were subsequently measured with a Guildline Autosal Laboratory Salinometer, Model 8400A. The absolute error in the CTD measurements is estimated as less than ± 0.025 psu (practical salinity units), $\pm 0.010^\circ\text{C}$ (temperature), and ± 1 m (depth).

Chlorophyll *a* fluorescence was profiled with a Seamartek in situ fluorometer protected with a light shield (Vincent et al. 1989) and mounted opposite the CTD on the rosette sampler. For absolute measurements of chlorophyll *a*, duplicate samples from each depth sampled for nutrients were filtered on to 4.25 cm diameter Whatman GF/F filters and stored frozen. The filters were subsequently ground in 90% acetone in a Teflon tissue grinder, the sample cleared by centrifugation, and then assayed for chlorophyll *a* by fluorometry before and after acidification (Strickland & Parsons 1972).

Duplicate samples for particulate nitrogen and phosphorus analysis were filtered through acid-washed, precombusted Whatman GF/F filters. These were subsequently Kjeldahl-digested and measured by auto-analyser as described in Vincent et al. (1989). The filtrates were analysed immediately for nutrients (nitrate plus nitrite, ammonium, urea) or were stored frozen for up to 2 months before analysis (silica, dissolved reactive phosphorus), using the auto-analytical methods detailed in Vincent et al. (1989).

Remote sensing data from the Advanced Very High Resolution Radiometer aboard the NOAA-9 and NOAA-11 satellites were received by the CSIRO Marine Laboratories facility in Hobart, Tasmania, Australia. Images were there processed to give sea surface temperature (SST) estimates using the method of McMillin & Crosby (1984) and remapped to a standard cartographic projection (Nilsson & Tildesley 1986). The SST values were calibrated using the near-surface (c. 2 m) CTD measurements during the cruise.

RESULTS

General distribution of water masses

A satellite mosaic of SST images from throughout Cruise 2027 emphasises the diverse range of water masses which surround the South Island (Fig. 2; for specific location names and general oceanographic

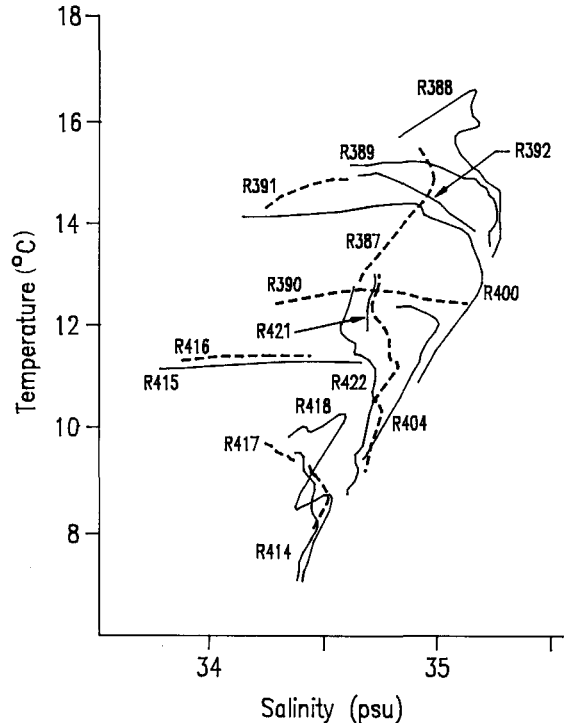


Fig. 3 Temperature-salinity plots for selected stations through the cruise. The curves are derived from the CTD profiles to 450 m, or to the sea floor if shallower than 450 m.

features see Fig. 1A and 1B). The ocean surface was 2–8° colder off the east coast relative to the west coast. Warm waters ($>16^\circ\text{C}$, coloured red) of the Subtropical Zone occurred to the west and north, with a band of cooler water (coloured yellow, 13.5–14.5°C) suggestive of upwelling along the Westland coast. From Fiordland southwards there was a gradual transition across the Subtropical Convergence (STC) into the cold (9°C) waters of the Subantarctic Zone. This frontal transition was diffuse to the west and south-west of the South Island, but was sharply defined along the south-eastern edge of the continental shelf. The STC lay parallel to the south-east coast of the South Island, and then turned eastwards at about 44°S , along the southern flank of the Chatham Rise. A band of cooler water extended northwards through the Mernoo Saddle, a depression west of Mernoo Bank (Fig. 1A). Large eddies and areas of diffuse mixing lay to the north and east of Mernoo Saddle. The cool Southland Current water (green, $12\text{--}13^\circ\text{C}$) was confined to the shelf between the STC (called the Southland Front in this region, Fig. 1B) and the

east coast, and continued northwards ultimately into Cook Strait.

The broad range of oceanic waters around the South Island is further indicated by the temperature-salinity plots for a selection of profiles throughout the cruise (Fig. 3). The plots show a gradation from cold, low-salinity subantarctic profiles (e.g., R414) to warm, high-salinity subtropical profiles (e.g., R388). The deep water T-S properties for all of the stations (with the exception of the Cook Strait profile, R387) lay along a straight line given by:

$$\text{Temperature} = -236 + 7.1 \text{ salinity.}$$

The surface water sections of the T-S plots demonstrated a variety of shapes, but in regions of freshwater influence (e.g., Stations R415 and R416 off the Clutha River; R400 off Doubtful Sound) the curves were almost horizontal, indicating the large dilution effect on salinity, but minimal influence on temperature.

Cook Strait front

The satellite image of Cook Strait (Fig. 4) showed that a sharp interface between warm seas to the north and the cold Southland Current water was positioned down the centre of the Strait, midway between the two islands (Fig. 4). The cooler southern water extended up to the middle of the Narrows. Further to the north in the Taranaki Bight region there were irregularly defined eddies where relatively cool (14°C, yellow on Fig. 4) west coast water appeared to be mixing with warmer northern subtropical water.

Water column profiles from Cook Strait also revealed large vertical gradients in many properties. Station R387 was located within the Narrows on the northern side of the front (Fig. 1). The CTD profiles

revealed at least six discrete strata each separated by pycnoclines of varying steepness (Fig. 5C). Warmest temperatures occurred in the uppermost layer, but a subsurface maximum in salinity occurred at about 140 m (Fig. 5B). In vivo fluorescence (Fig. 5C) and chlorophyll *a* concentrations (Fig. 5A) rose sharply to a maximum at about 25 m depth, then gradually declined to low background values at 100 m. Nitrate (Fig. 5A) and DRP (not shown) rose with depth down the water column, with the sharpest rise beneath 100 m. Even the surface waters, however, were rich in nitrate and other nutrients (Table 1). The concentration of ammonium and urea, as at all other stations except in Foveaux Strait (see below), remained at or below our analytical limit of 0.05 mmol m⁻³. The particulate N:P ratios were high throughout the water column and indicative of surplus nitrogen relative to phytoplankton growth requirements.

West coast upwelling

The SST images showed a band of cold water extended along much of the western coastline of the South Island during the period of the cruise (Fig. 2, 4, and 6). The coldest temperatures (< 13°C, blue in Fig. 6) were in the inshore waters immediately adjacent to the coast. The outer region of this band was 1–2°C warmer and it was irregularly shaped into a series of breaking wave-like plumes. One of the largest of these extended about 40 km out from the coastline off Abut Head. A series of profiles were obtained near the centre of this feature (at 43°S, 170°E) 12 h after the SST image in Fig. 6. The CTD profiles (Fig. 7B) showed that the 15°C surface temperature was associated with a mixed layer of reduced salinity that extended to about 30 m depth.

Table 1 Near-surface water properties at Cook Strait Station R387, and at stations off the West Coast of the South Island. All samples were at 10 m (except R400, 5 m), 16–21 May 1989. All concentrations are in mmol m⁻³ unless otherwise noted. The ratios are molar.

Station	Temperature (°C)	Salinity (psu)	Nutrients				Particulates			
			NO ₃	DRP	N:P	Si	N	P	N:P	Chl. <i>a</i> (mg m ⁻³)
R387	15.41	34.92	3.2	0.41	7.9	2.9	0.91	0.05	18.2	0.30
R388	15.72	34.85	0.0	0.11	0.0	1.3	0.78	0.05	15.6	0.29
R389	15.19	34.61	0.4	0.17	2.3	1.8	0.76	0.05	15.2	0.43
R390	14.60	34.62	2.8	0.25	11.0	2.5	1.01	0.14	7.2	0.41
R391	14.49	34.31	1.5	0.26	5.7	1.9	0.97	0.08	12.1	0.71
R392	14.94	34.68	0.9	0.16	5.9	1.6	0.92	0.06	15.3	0.70
R393	14.56	34.09	0.7	0.20	3.3	2.1	1.07	0.06	17.8	0.53
R400	14.17	34.28	0.4	0.18	2.2	2.2	1.11	0.06	18.5	0.52

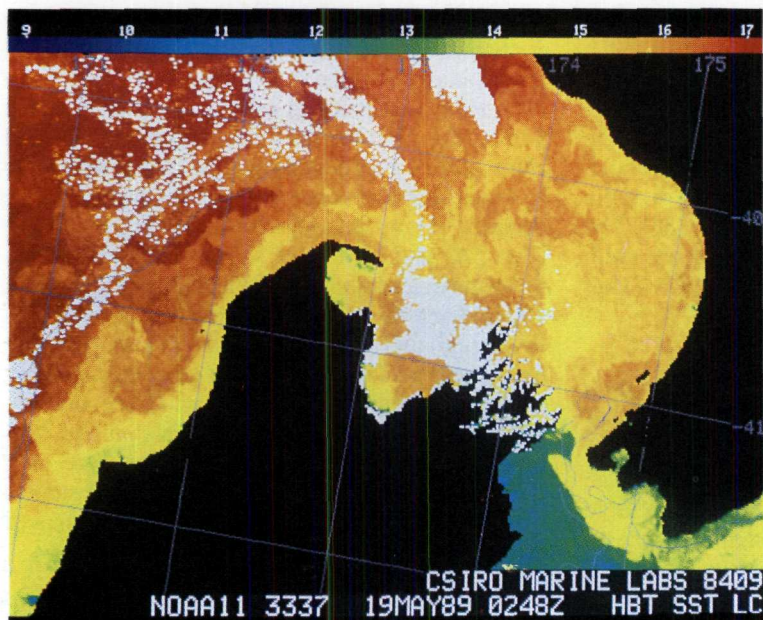


Fig. 4 SST image for the Cook Strait-Taranaki Bight region, 19 May 1989.

Chlorophyll *a* (Fig. 7A) peaked midway down this surface layer and overlaid a region of rapidly increasing density (Fig. 7C) and nitrate concentration (Fig. 7A). Even in the near-surface waters, however, nitrate concentrations were at or above 1 mmol N m^{-3} .

A larger but similarly shaped plume can be seen in the SST image in Fig. 4 centred at about 41.5°S , 171.5°E . It extended about 70 km northwards from the Buller River into the Karamea Bight, and pointed in the opposite direction to that off Abut Head, suggesting the different directions of alongshore flow

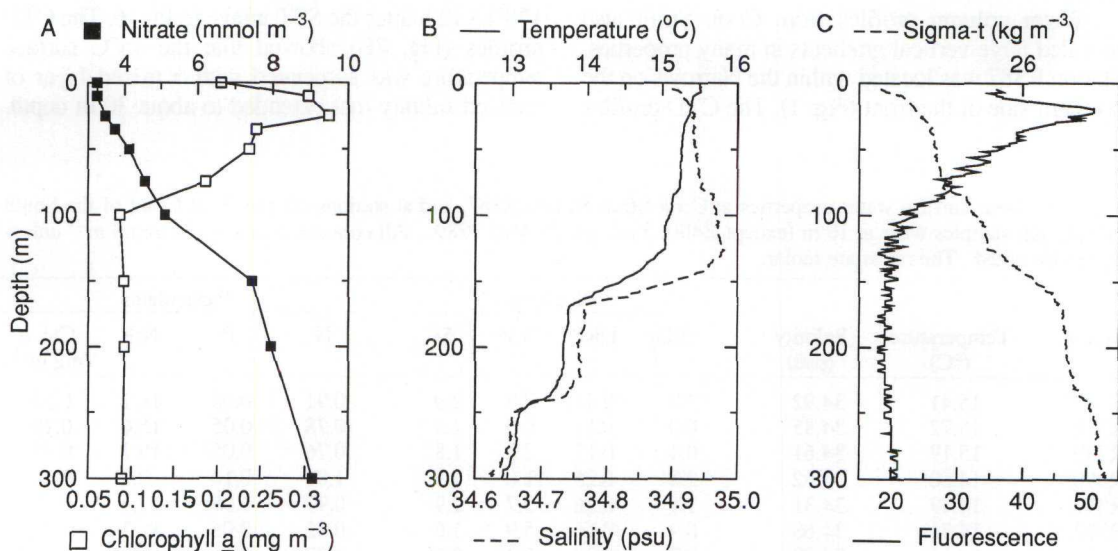
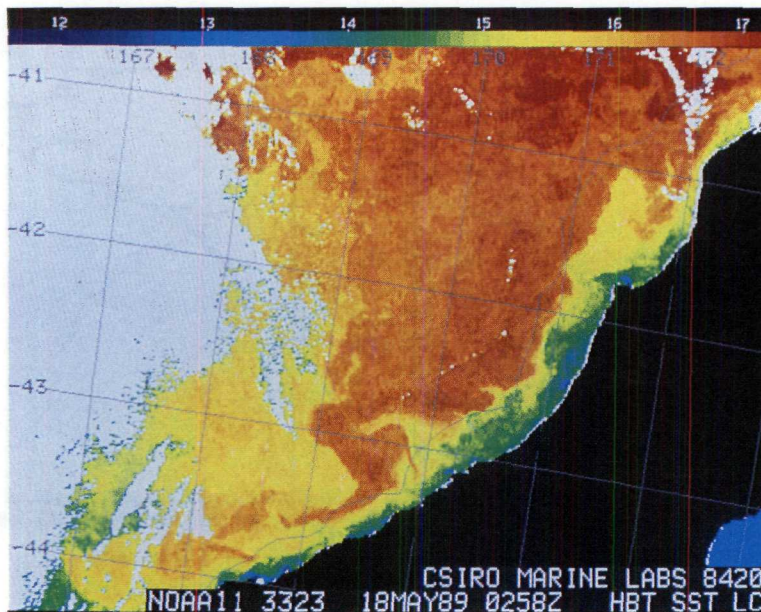


Fig. 5 Water column properties at Station R387 in The Narrows, Cook Strait, 16 May 1989.

Fig. 6 SST image for the West Coast region, 18 May 1989.



at these two widely separated (c. 200 km) locations. The same feature is discernible, but less sharply defined, in the SST image taken one day earlier (Fig. 6). Our water column sampling in Karamea Bight was c. 12 h before the Fig. 6 image, and three of our stations are likely to have been within the

plume at various distances from the Buller River mouth: Station R388 (75 km), R389 (17 km), and R390 (7 km). The CTD-F profiles at Station R388 revealed a vertical structure similar to that observed in the plume off Abut Head. A surface layer of cool low-salinity water extended to about 20 m depth and

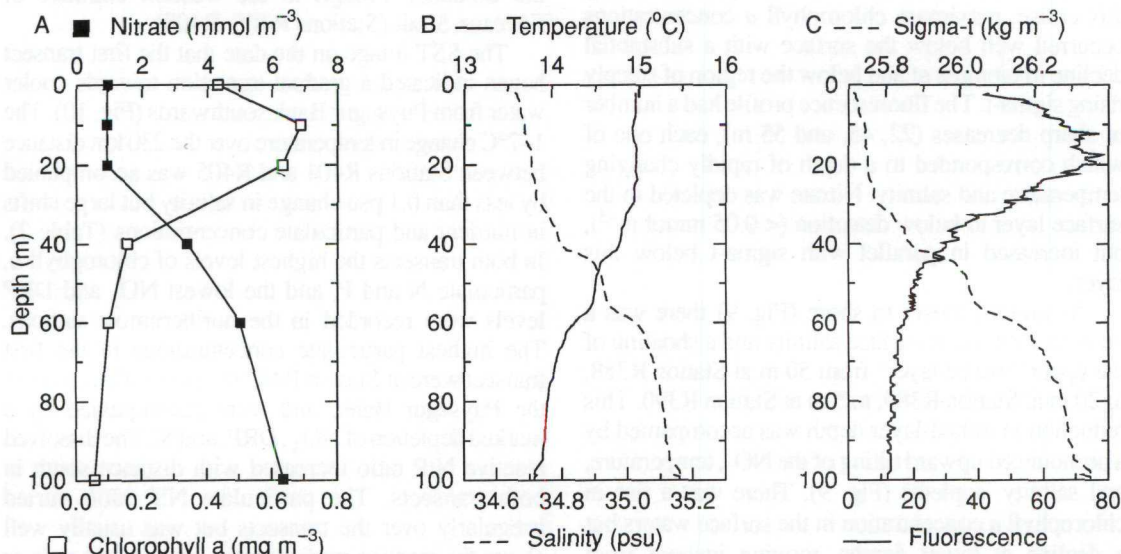


Fig. 7 Water column properties in the plume off Abut Head, Station R392, 18 May 1989.

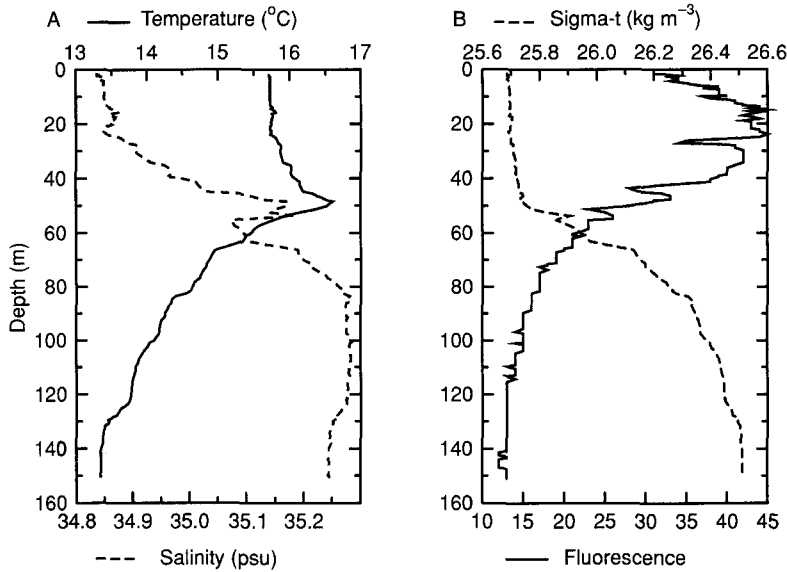


Fig. 8 Water column properties in the plume off the Buller River, Station R388, 17 May 1989.

overlaid a region of increasing salinity and temperature (Fig. 8). Both variables rose to well-defined maxima at around 50 m. The salinity values fell to a secondary minimum at 60 m, with a third minimum in the well-mixed band of water at the base of the water column. The sigma-t profile was relatively flat to 50 m, suggesting that the temperature and salinity structure above that depth could be readily disrupted by mixing. As recorded in all of the west coast profiles during this cruise, maximum chlorophyll *a* concentrations occurred well below the surface with a substantial decline in biomass at and below the region of steeply rising sigma-t. The fluorescence profile had a number of sharp decreases (22, 45, and 55 m), each one of which corresponded to a depth of rapidly changing temperature and salinity. Nitrate was depleted in the surface layer to below detection ($< 0.05 \text{ mmol m}^{-3}$), but increased in parallel with sigma-t below this layer.

At stations closer to shore (Fig. 9) there was a marked decrease in surface salinity and a shoaling of the upper "mixed layer" from 50 m at Station R388, to 20 m at Station R389, to 5 m at Station R390. This reduction in mixed-layer depth was accompanied by a pronounced upward tilting of the NO_3 , temperature, and salinity isopleths (Fig. 9). There was a rise in chlorophyll *a* concentration in the surface waters but a decline at lower depths, moving inshore from Stations R388 to R389.

South-western transects

Two transects were sampled to examine the north-south gradient in oceanographic properties off the south-western corner of the South Island. The first transect extended from Puysegur Bank (Station R401, west of Puysegur Point, Fig. 1A) across the Solander Trough (R404) to Snares Island (R405), and the second from Snares Island along the eastern edge of the Solander Trough to the western entrance of Foveaux Strait (Stations R405–R408).

The SST image on the date that the first transect began indicated a gradual transition towards cooler water from Puysegur Bank southwards (Fig. 10). The $1\text{--}2^\circ\text{C}$ change in temperature over the 230 km distance between Stations R401 and R405 was accompanied by less than 0.1 psu change in salinity but large shifts in nutrient and particulate concentrations (Table 2). In both transects the highest levels of chlorophyll *a*, particulate N and P, and the lowest NO_3 and DRP levels were recorded in the northernmost stations. The highest particulate concentrations in the first transect were at Station R402 off the southern side of the Puysegur Bank, and were accompanied by a marked depletion of NO_3 , DRP, and Si. The dissolved reactive N:P ratio increased with distance south in both transects. The particulate N:P ratio varied irregularly over the transects but was usually well above the reactive nutrient ratio, and always near or above the Redfield ratio of 15.5:1.

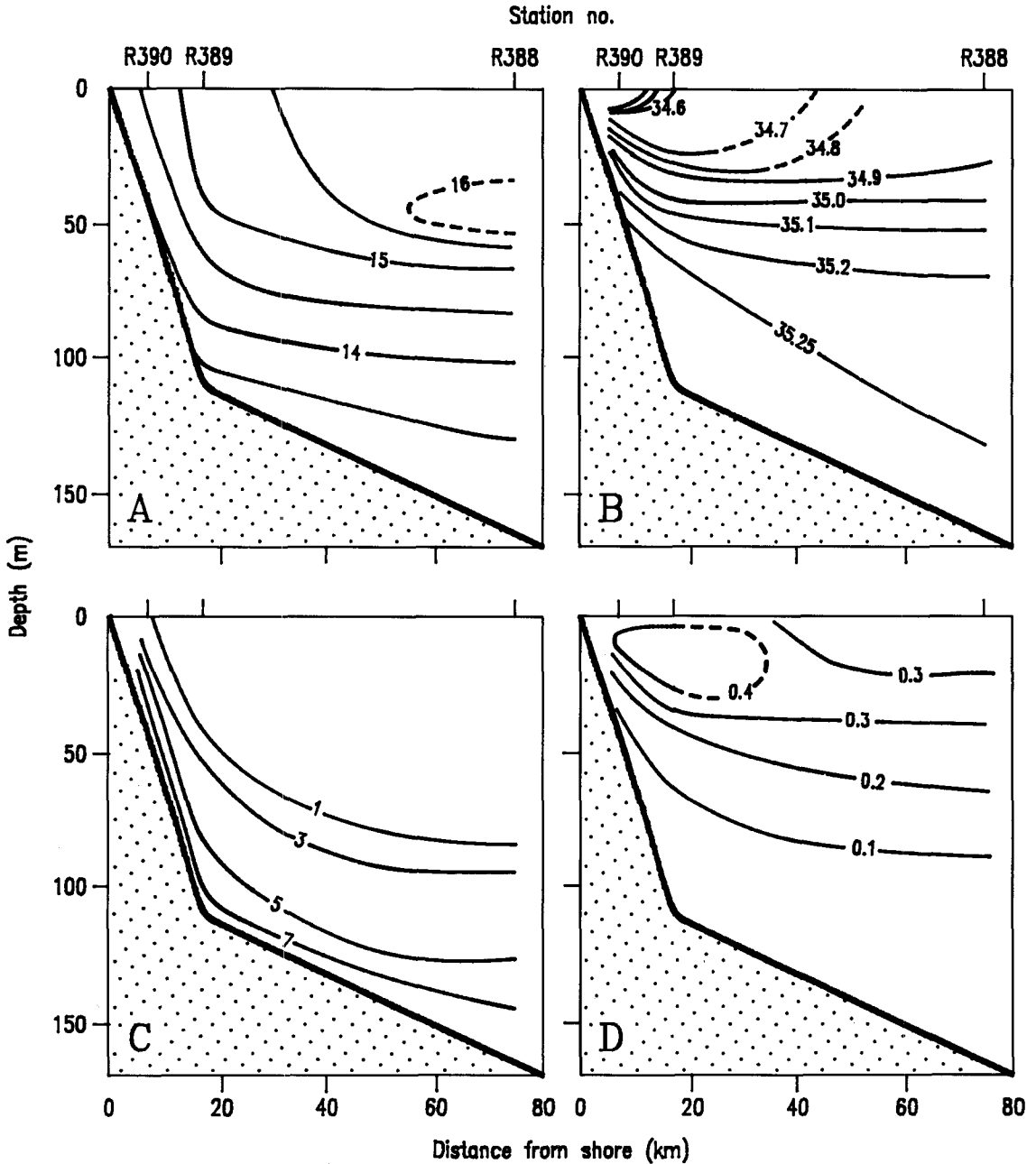


Fig. 9 Temperature (A, in °C), salinity (B, in psu), nitrate (C, in mmol m^{-3}) and chlorophyll *a* (D, in mg m^{-3}) sections through the plume off the Buller River, 17 May 1989.

Foveaux Strait

The temperature and salinity transects through Foveaux Strait (Table 3) showed a transition from warm, saline water at Station R408 in the west to

slightly cooler and less saline water at Station R413 in the east, consistent with the pattern suggested by the SST images (Fig. 2 and 10). The east-west gradients within Foveaux Strait were relatively weak

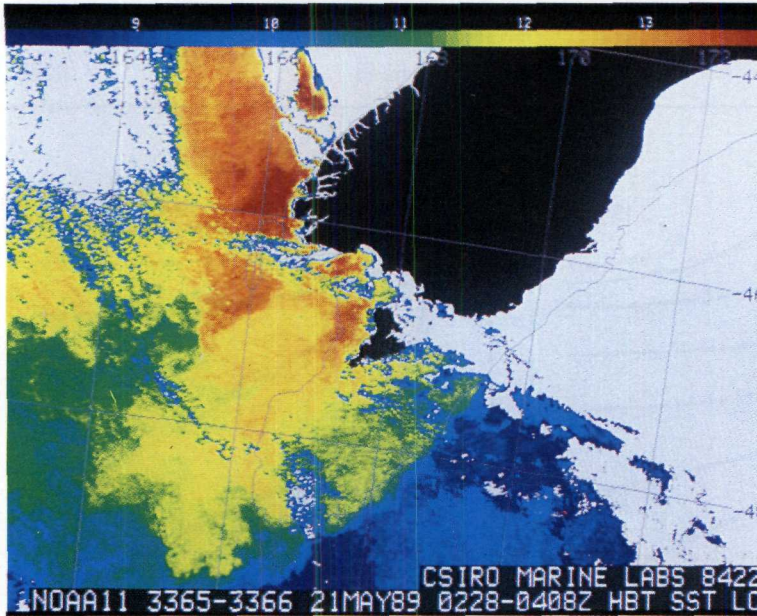


Fig. 10 Composite of 2 SST images for the southern South Island region, 21 May 1989.

in all properties, except for nitrate which doubled in concentration between Stations R412 and R413. Particulate N varied from 0.4 to 0.9 mmol m⁻³ with no consistent trend through the Strait. The particulate N:P ratios were at or above the Redfield ratio of 15.5:1, with the exception of Stations R409 and R410. The latter had a noticeably lower temperature and salinity relative to the surrounding waters and an elevated silica content. It was a site closest to the South Island coast and may have been influenced by

riverine discharges, particularly from the Aparima and Oreti Rivers.

The profiling at each of the stations in Foveaux Strait revealed a homogeneous distribution of properties indicative of strong vertical mixing. The in vivo fluorescence values varied by less than 5% down the water column at each station. However, at most of the stations (R408–R412) there was a small rise in ammonium (Fig. 11) and sometimes urea and DRP towards the base of the water column.

Table 2 Near-surface properties of the ocean across the two south-western transects. All samples and measurements were at 10 m, 21–24 May 1989. All concentrations are in mmol m⁻³ unless otherwise noted. The ratios are molar. Note that Station R405 forms the southern end of both transects.

Station	Temperature (°C)	Salinity (psu)	Dissolved nutrients				Particulates			
			NO ₃	DRP	N:P	Si	N	P	N:P	Chl. <i>a</i> (mg m ⁻³)
R401	13.73	34.89	2.8	0.24	11.6	1.4	0.58	0.03	18.7	0.32
R402	13.82	34.88	0.9	0.08	11.6	0.7	0.91	0.05	17.2	0.46
R403	13.13	34.92	4.0	0.41	9.7	1.5	0.61	0.04	14.9	0.42
R404	12.37	34.82	5.1	0.38	13.3	1.7	0.50	0.03	16.7	0.24
R405	11.97	34.77	6.5	0.36	17.9	1.6	0.42	0.02	21.0	0.17
R408	12.98	34.82	2.6	0.32	8.1	1.1	0.90	0.05	17.6	0.47
R407	13.22	34.89	3.1	0.37	8.3	1.3	0.48	0.03	16.5	0.14
R406	12.04	34.77	6.9	0.61	11.4	2.1	0.38	0.02	19.6	0.22
R405	11.97	34.77	6.5	0.36	17.9	1.6	0.42	0.02	21.0	0.17

Subtropical versus subantarctic profiles

The SST images (e.g., Fig. 2) emphasised the large difference in surface temperatures between the subtropical and subantarctic water masses. The major contrasts between waters to the north and south of the STC is seen by a comparison of profiles from two offshore, geographically well-separated stations: R414 in the subantarctic zone and R422 in the subtropical zone (Fig. 12). Stratification was weakly established in the subantarctic relative to the subtropical profile, with a $\Delta \sigma_t$ between 50 and 150 m of $< 0.1 \text{ kg m}^{-3}$ at R414 and $> 0.3 \text{ kg m}^{-3}$ at R422. The mixed layer was slightly shallower at Station R422 (c. 70 m) with substantial depletion of nitrate and much higher chlorophyll *a* concentrations relative to Station R414 (mixed-layer depth of 100 m). The in vivo fluorescence profiles were relatively homogeneous to 75 m at both stations, indicating strong vertical mixing at these exposed oceanic sites. However, it is also of interest that the strength of the fluorescence signal was very similar in the two waters despite their markedly different chlorophyll *a* content (see below). The completely different T-S signatures of the two profiles (Fig. 3), with cool low-salinity water at Station R414 and warm high-salinity water at Station R422 underscores the major physical contrast between these two oceanic zones.

STC over the Chatham Rise

A satellite image taken on 22 May 1989, 3 days before the transect over Chatham Rise, showed that the transition from subantarctic to subtropical water occurred across a dynamic irregularly shaped frontal zone (Fig. 13). A plume of cold (11–12°C) water (coloured pale blue) streamed northwards over the Mernoo Saddle. Further eastwards over the crest and

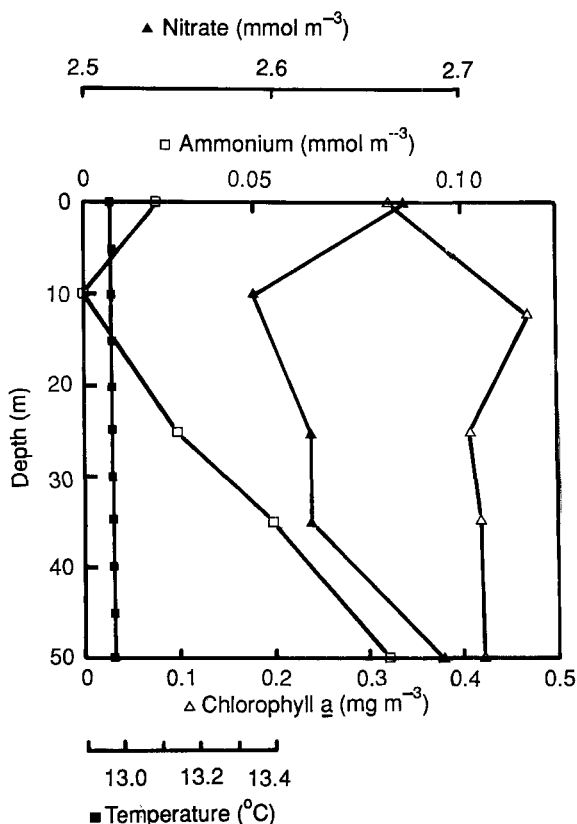


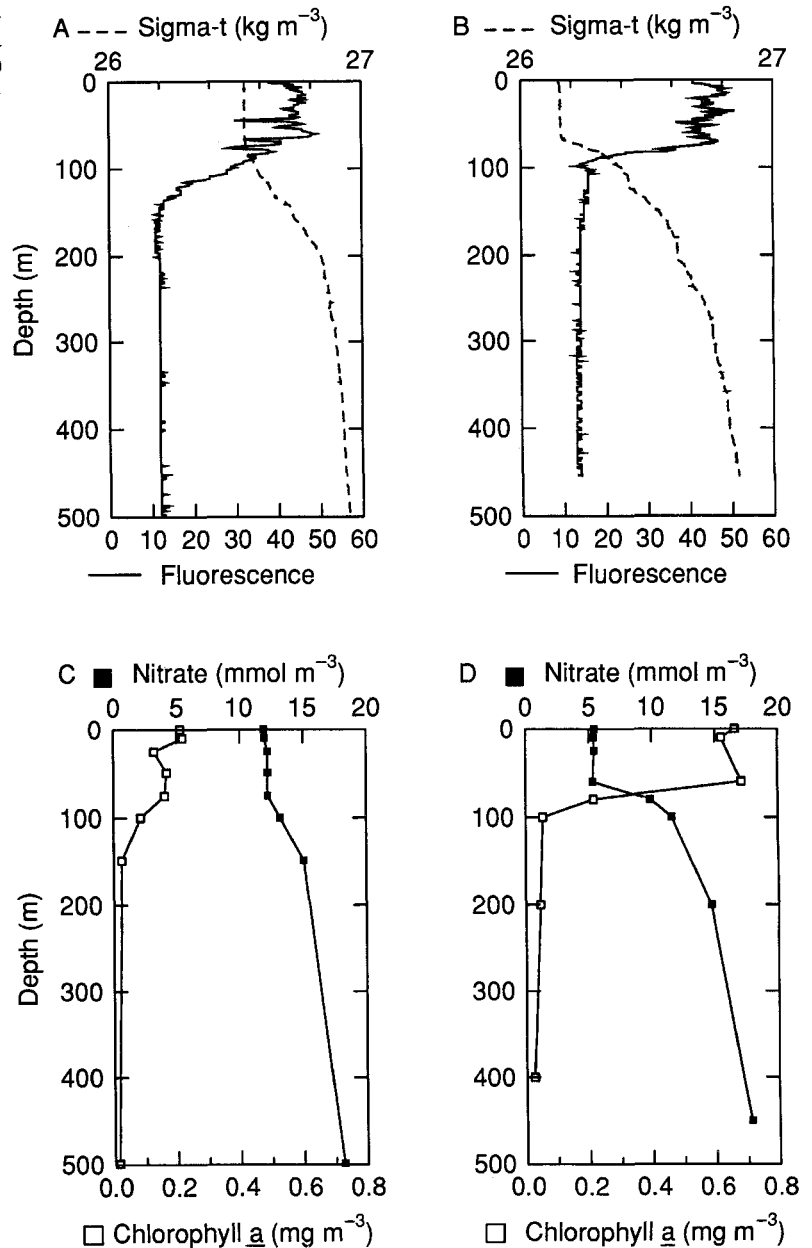
Fig. 11 Water column profiles at Station R408 at the western end of Foveaux Strait, 24 May 1989.

to the north of the rise the temperature fluctuations were complicated by a number of large circular patches of water that were 1–2°C warmer than the surrounding ocean. The largest and also warmest of these was centred at c. 42.3°S, 176.0°E and was

Table 3 Near-surface properties through Foveaux Strait, with comparative data for further west (R401) and east (R414). All samples were at 10 m, 22–25 May 1989. All concentrations are in mmol m^{-3} unless otherwise noted. The ratios are molar.

Station	Temperature (°C)	Salinity (psu)	Dissolved nutrients				Particulates			
			NO ₃	DRP	N:P	Si	N	P	N:P	Chl. <i>a</i> (mg m ⁻³)
R401	13.73	34.89	2.8	0.24	11.6	1.4	0.58	0.03	18.7	0.32
R408	12.98	34.82	2.6	0.32	8.1	1.1	1.1	0.05	17.6	0.47
R409	12.47	34.76	3.4	0.41	8.3	1.2	0.64	0.04	16.1	0.38
R410	11.96	34.54	3.3	0.40	8.3	1.5	0.43	0.04	10.5	0.34
R411	12.14	34.70	3.2	0.24	13.1	1.2	0.52	0.04	13.0	0.26
R412	11.95	34.62	3.3	0.27	12.3	1.5	0.52	0.03	16.1	0.29
R413	11.61	34.72	6.1	0.43	14.1	1.8	0.72	0.04	18.0	0.33
R414	9.50	34.36	12.0	0.76	15.8	2.3	0.65	0.04	16.3	0.22

Fig. 12 Comparison of sub-antarctic (A, C: Station R414) and subtropical (B, D: Station R422) water column profiles, 25 and 28 May 1989.

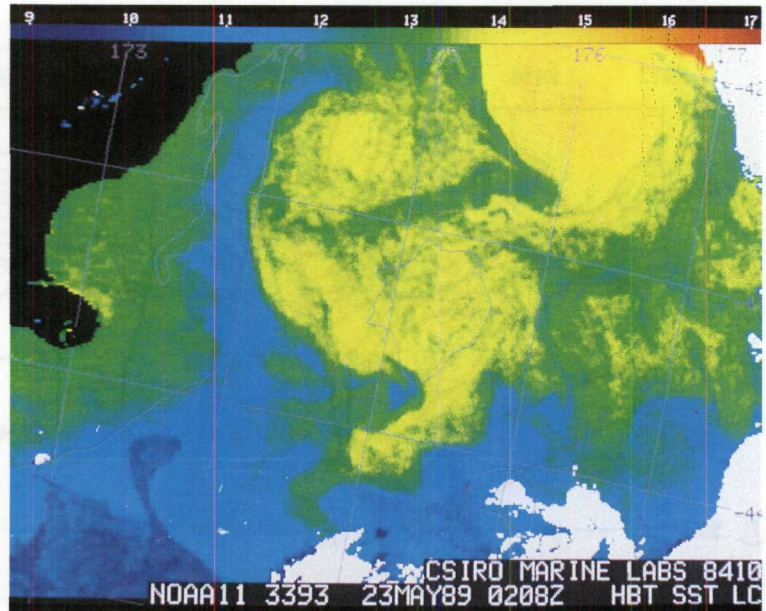


c. 110 km across. A second patch was centred exactly over the Mernoo Bank and appeared to be connected to a stream of warm water moving southward into the frontal zone. A third circular patch was centred at c. 42.6°S, 174.5°E (Fig. 13, Fig. 1B) just north-west of Mernoo Bank.

The cruise transect across Chatham Rise was broadly consistent with these SST observations. The sharpest temperature change was around 44°S, well

south of the crest of the rise (Fig. 14A). A change in salinity of c. 0.4 psu accompanied this temperature gradient (Fig. 14B). The circular feature centred over Mernoo Bank contained well-mixed, moderately warm (c. 13°C), saline (c. 34.72 psu) water and was bounded to the north and south by cooler, less-saline water. The mixed layer deepened to c. 100 m over Mernoo Bank from < 70 m in adjacent stations (R417 and R422). A tongue of high-salinity water (up to

Fig. 13 SST image for the Mernoo Saddle-Chatham Rise region, 23 May 1989. Note the position of Mernoo Bank at 43.5°S, 175.5°E demarcated by the 200 m isobath.



34.8 psu) extended from the southern side of the rise at about 200 m depth. This water gradually decreased in salinity, cooled, and deepened as it moved southwards. This feature was still well defined 150 km from Mernoo Bank, but at c. 200 km (Station R417) was no longer discernible.

The eddy-like circular feature over Mernoo Bank can also be resolved in the nutrient and particulate data as a region of slightly higher nitrate and reduced chlorophyll *a* (Fig. 14C and 14D). Highest chlorophyll *a* concentrations were recorded well south of the rise at Station R419, within the frontal region of most rapid temperature and salinity change. The core of

elevated chlorophyll *a* (up to 1.5 mg m^{-3}) lay immediately above a tongue of low-salinity subantarctic water that was at about 60 m depth.

A comparison of nutrients and particulates at 10 m depth shows the large but irregular variations from south to north in oceanographic properties (Table 4). Silica, nitrate, and DRP were substantially reduced at Station R419 relative to R414 and approached concentrations comparable with waters much further to the north (Stations R422, R423). Inorganic as well as particulate N:P ratios were highest in the south with an abrupt fall in particulate N:P at the stations of highest chlorophyll *a*, R419 and R422. Particulate

Table 4 Distribution of oceanographic properties off the East Coast of the South Island from south to north. All samples were at 10 m. 25–28 May 1989. –, no data. All concentrations are in mmol m^{-3} unless otherwise noted. The ratios are molar.

Station	Temperature (°C)	Salinity (psu)	Dissolved nutrients				Particulates			
			NO ₃	DRP	N:P	Si	N	P	N:P	Chl. <i>a</i> (mg m^{-3})
R414	9.50	34.36	12.0	0.76	15.8	2.3	0.65	0.04	16.3	0.22
R417	9.73	34.25	12.1	–	–	–	0.85	0.05	17.1	0.24
R418	9.82	34.34	11.8	–	–	–	0.72	0.05	14.4	0.30
R419	11.73	34.51	7.2	0.55	12.7	0.9	1.15	0.08	13.6	1.46
R420	13.08	34.72	5.5	–	–	–	0.74	0.05	14.5	0.51
R421	13.05	34.71	6.5	–	–	–	0.60	0.04	16.9	0.27
R422	12.74	34.63	5.4	0.49	11.0	1.3	0.77	0.05	15.4	0.62
R423	11.85	34.63	6.1	0.55	11.1	1.0	1.27	0.09	13.6	0.88

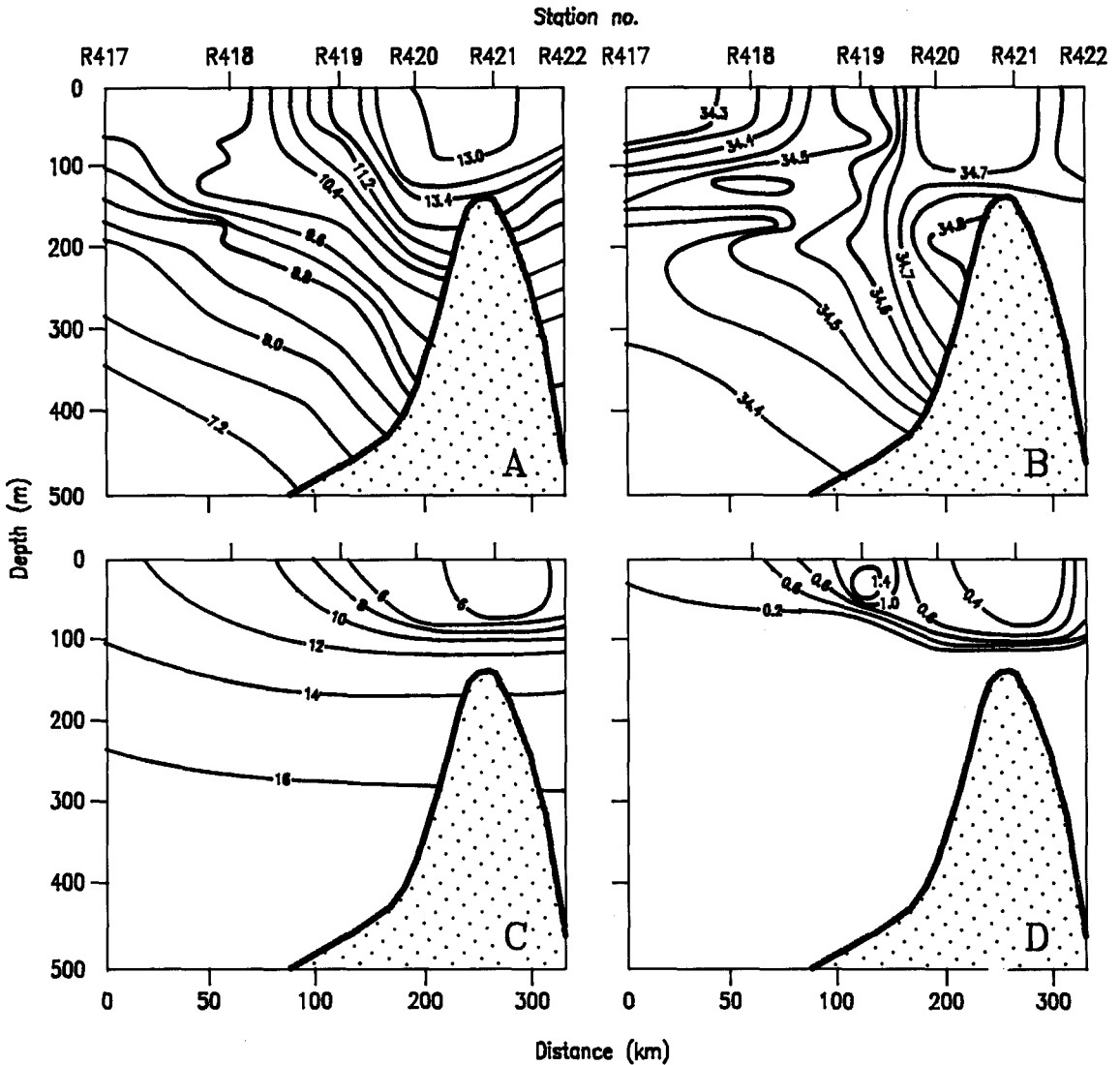


Fig. 14 Temperature (A, in °C), salinity (B, in psu), nitrate (C, in mmol m^{-3}) and chlorophyll *a* (D, in mg m^{-3}) sections across the Chatham Rise along longitude 175°E, 25–28 May 1989.

N:P ratios were much higher in the water over Mernoo Bank (Stations R420, R421) than at adjacent stations.

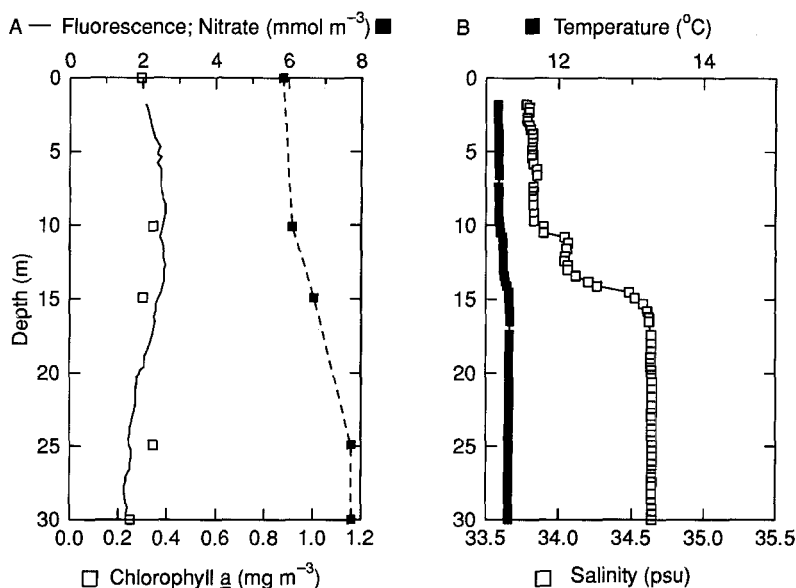
Inshore waters

Many of the stations sampled inshore near the east as well as west coast of the South Island were strongly influenced by freshwater inputs to the sea. Although the surface water salinities were rarely diluted below 34.0 psu there were major changes in the physical structure of the water column, with a surface mixed

layer of 5 m (e.g., Station R390) to 10 m (e.g., Station R415) overlying a strong pycnocline of rising salinity. These thin surface inshore layers were slightly cooler than the water beneath, but the temperature difference was rarely more than 0.3°C (e.g., off the Clutha River, Fig. 15).

Multiple pycnoclines were a feature of many of the inshore profiles, for example, at 10 m and 14 m at the Clutha River offshore station (Fig. 15). This multiple layering was especially conspicuous off Thompson Sound (Station R393) and Doubtful Sound

Fig. 15 Water column properties at Station R416, off the Clutha River, 25 May 1989.



(Station R400, Fig. 16) where the freshwater outflows were discharged into a deep water column. A surface layer of gradually rising salinity and temperature overlaid a sharp pycnocline at 10–20 m depth, with a second pycnocline at the base of the offshore mixed layer, at about 90 m. The fluorescence profiles indicated a sharp minimum in chlorophyll *a* concentrations at the base of the upper pycnocline.

Nutrient and particulate concentrations were highly variable between the inshore stations but chlorophyll *a* values inshore were often higher than at adjacent sites further from the coast (Table 5). Silica levels were higher than in surface water offshore and at deeper inshore depths, reflecting the input of terrigenous nutrients. Some of the dissolved inorganic

N:P ratios in these surface waters were among the lowest recorded during the cruise (e.g., 1.9 at Station R391), but the particulate N:P ratios were often much higher and bore little relationship to the nutrients.

General relationships between properties

Several significant correlative relationships were observed between the oceanographic variables measured in this study. Table 6 gives the correlation coefficients for the surface mixed-layer data presented in Tables 1–5. Nitrate and DRP, and also their ratio, were significantly and inversely correlated with temperature reflecting the high nutrient content of the cool subantarctic waters, and the tendency towards nitrate depletion (to a greater extent than DRP

Table 5 Surface water properties at inshore sites around the South Island, 17–25 May 1989. Samples and measurements were in the depth range 0–2 m. The number in parentheses is the distance from shore in km. All concentrations are in mmol m⁻³ unless otherwise noted. The ratios are molar.

Station	Temperature (°C)	Salinity (psu)	Dissolved nutrients				Particulates			
			NO ₃	DRP	N:P	Si	N	P	N:P	Chl. <i>a</i> (mg m ⁻³)
R390 (7.8)	14.403	34.317	2.7	0.29	9.3	2.8	1.18	0.16	7.3	0.32
R391 (5.7)	14.340	34.245	0.3	0.16	1.9	2.0	1.81	0.13	13.9	0.86
R393 (2.6)	14.570	34.088	0.7	0.22	3.2	2.4	1.52	0.08	19.1	0.44
R400 (4.4)	14.162	34.240	0.4	0.19	2.1	2.2	1.13	0.07	16.1	0.46
R415 (15.6)	11.165	33.799	5.8	0.46	12.6	3.1	1.06	0.07	15.1	0.29
R416 (5.0)	11.365	33.903	5.3	0.32	16.6	4.0	1.41	0.13	10.4	0.62

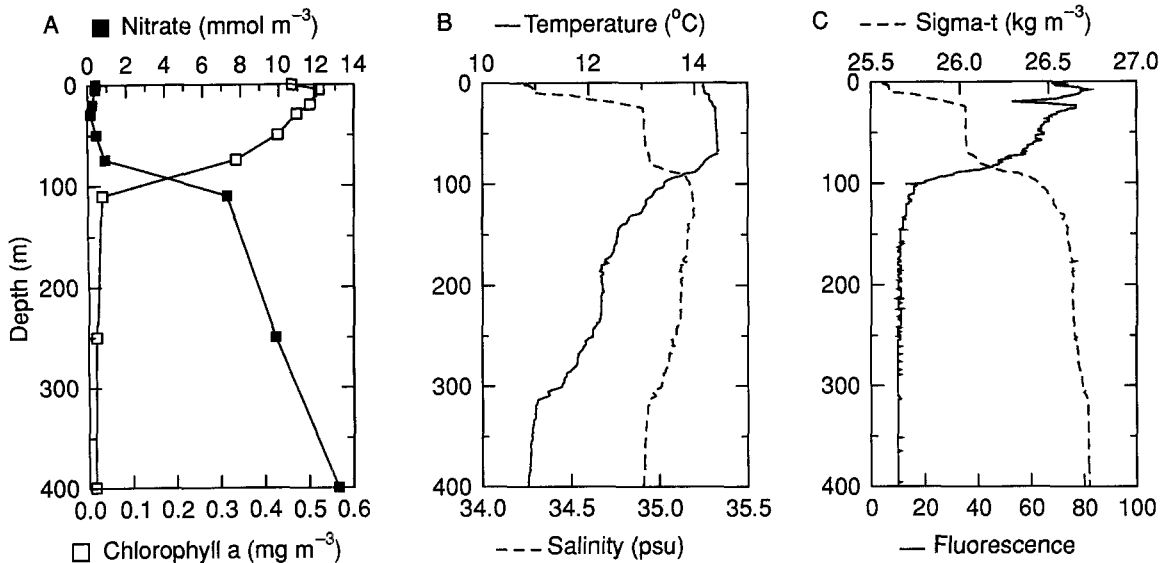


Fig. 16 Water column properties at Station R400 off Doubtful Sound, 21 May 1989.

depletion) in the warmer subtropical waters. Silica did not show the same effect, but was inversely correlated with salinity, indicative of the freshwater influence on both variables. A similar inshore effect showed up in the inverse correlation between particulate N and P, and salinity. These elemental particulate concentrations were uncorrelated with dissolved nutrients but were correlated directly with chlorophyll *a*. The particulate N:P ratios showed no relationship to the dissolved-nutrient ratios, but correlated significantly with the particulate-phosphorus concentrations.

As a further guide to planktonic biomass at each station, the total water column content of chlorophyll

a was estimated by trapezoidal integration down to the depth of background chlorophyll *a* fluorescence. The integral biomass ranged from 5 to 10 mg Chl. *a* m⁻² at the shallow sites (e.g., R409–R412 in Foveaux Strait), to > 50 mg Chl. *a* m⁻² at certain oceanic stations (maximum of 88.2 mg Chl. *a* m⁻² at R419). The integral biomass estimates correlated with the near-surface Chl. *a* concentration (but *r*² only 0.422), and there was no significant correlation with any other measured variable.

The correlation analysis was subsequently repeated for an offshore subset of the data to determine whether there were similar relationships between variables for a specific group of deep oceanic stations.

Table 6 Correlation matrix for the oceanographic properties of the surface mixed layer using the data in Tables 1 to 5. T = temperature, S, salinity; PN and PP, particulate N or P; N, NO₃-N; P, DRP; Si, silica; ΣChl. *a*, integral Chl. *a*. Only correlations at *P* < 0.05 are given.

	T	S	N	P	Si	N:P	Chl. <i>a</i>	PN	PP	PN:PP	ΣChl. <i>a</i>
T	1.00										
S	–	1.00									
N	–0.87	–	1.00								
P	–0.78	–	0.93	1.00							
Si	–	–0.61	–	–	1.00						
N:P	–0.79	–	0.80	0.60	–	1.00					
Chl. <i>a</i>	–	–	–	–	–	–	1.00				
PN	–	–0.66	–	–	0.39	–	0.57	1.00			
PP	–	–0.41	–	–	–	–	0.52	0.75	1.00		
PN:PP	–	–	–	–	–	–	–	–	–0.58	1.00	
ΣChl. <i>a</i>	–	–	–	–	–	–	0.65	–	–	–	1.00

The data set was restricted to 8 stations 100 km or more off the east coast of the South Island: R414 and R417–R423. This subset therefore encompassed the strong gradients across the STC and over Chatham Rise, but minimised any coastal and east–west effects. This analysis identified many of the same correlative relationships as in the overall data set (Table 7). Temperature and salinity were closely correlated with each other, and inversely with nutrients. There was an extremely close inverse relationship between temperature and DRP ($r^2 = 0.996$) but less precise inverse correlations with NO_3 ($r^2 = 0.921$), silica ($r^2 = 0.672$), and NO_3/DRP ratio ($r^2 = 0.903$). The salinity effect on silica and particulates was no longer significant, further supporting the conclusion that this was a coastal effect in the full data set (see above). In addition to correlations with the other estimates of particulate concentration, Chl. *a* was significantly and inversely related to particulate N:P ratios; at the higher biomass concentrations the seston was depleted in N relative to P. Integral Chl. *a* was much more closely correlated with surface concentrations of this pigment than in the overall data set, and also to particulate N and P. As with the full analysis, there was no relationship with nutrients, temperature, or salinity. None of the descriptors of biological particulates correlated with the physical or chemical-state variables (Table 7).

In vivo chlorophyll *a* fluorescence

The in vivo fluorescence profiles through the cruise provided an excellent guide to the detailed vertical distribution of phytoplankton, and at any single station there was usually a close relationship between fluorescence and chlorophyll *a* (e.g., $r = +0.89$ for R414; $+0.98$ for R419; $+0.94$ for R388). However,

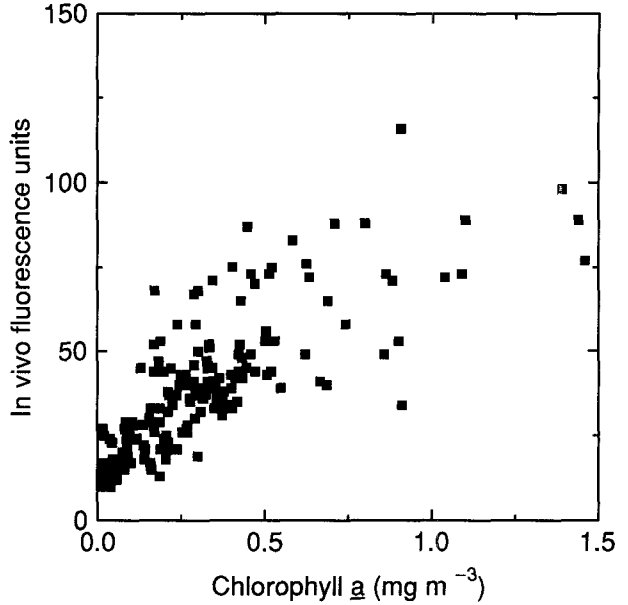


Fig. 17 In vivo fluorescence (instrument units) against extracted chlorophyll *a* concentrations for all stations and depths.

this relationship was much less precise between stations. For example, the least-squares regression curve for fluorescence (*F*) was:

$F = 12.36 + 152.3 \text{ Chl. } a$ for the profile at R414 but $F = 10.9 + 54.2 \text{ Chl. } a$ at R419. For the cruise data at all depths and stations ($n = 188$) the correlation coefficient was $+0.76$ (Fig. 17), and for the 10 m data in Tables 1–5 the coefficient dropped to $+0.56$.

To examine whether there was an influence of surface bright light on fluorescence yield the fluorescence per unit Chl. *a* ($F_{\text{Chl. } a}$) was calculated

Table 7 Correlation matrix for the oceanographic properties of the surface mixed layer for the Chatham Rise transect (Stations R417–R423), plus Station R414. T, temperature; S, salinity; PN and PP, particulate N or P; N, $\text{NO}_3\text{-N}$; P, DRP; Si, silica; $\Sigma\text{Chl. } a$, integral Chl. *a*. Only correlations at $P < 0.05$ are given.

	T	S	N	P	Si	N:P	Chl. <i>a</i>	PN	PP	PN:PP	$\Sigma\text{Chl. } a$
T	1.00										
S	0.96	1.00									
N	-0.96	-0.95	1.00								
P	-1.00	-0.93	0.99	1.00							
Si	-0.82	-0.79	0.88	0.86	1.00						
N:P	-0.95	-0.99	0.99	0.96	—	1.00					
Chl. <i>a</i>	—	—	—	—	—	—	1.00				
PN	—	—	—	—	—	—	0.78	1.00			
PP	—	—	—	—	—	—	0.82	0.99	1.00		
PN:PP	—	—	—	—	—	—	0.73	—	-0.80	1.00	
$\Sigma\text{Chl. } a$	—	—	—	—	—	—	0.94	0.85	0.89	—	1.00

for 0 m and 10 m at each site, and then the 0 m $F_{\text{Chl. } a}$ was divided by the 10 m value. These ratios were then split into two groups: stations sampled during daylight hours and at night. There was no significant difference between these latter two groups, with the depth ratios averaging 0.95 (SD = 0.18) in the day and 1.07 (SD = 0.37) at night. However, the lowest ratios were recorded in the daytime data set (minimum of 0.68 at Station R391), suggesting surface inhibition at certain stations.

The correlation analysis was then extended to examine the relationship between $F_{\text{Chl. } a}$ at 10 m and the other oceanographic variables. In the overall cruise data set there was a significant positive correlation with nitrate (+0.52), and significant negative correlations with Chl. *a* (-0.51), integral Chl. *a* (-0.58), and temperature (-0.54). Over the Chatham Rise transect (Stations R414, R417-R423) $F_{\text{Chl. } a}$ was highest in the south (maximum of 205 at Station R414), and low in the north (79 at Station R422), and correlated strongly with the gradients in other oceanographic variables across this region. The correlation was positive with NO_3 (0.91), DRP (0.92), silica (0.98), nutrient ratios (0.85), and particulate ratios (0.64); it was negative with temperature (-0.84), salinity (-0.84), chlorophyll *a* (-0.72), particulate nitrogen (-0.41), particulate phosphorus (-0.50), and integral chlorophyll *a* (-0.80).

DISCUSSION

The temperature, salinity, and surface nutrient data presented here are broadly consistent with previous studies at specific sites around the South Island (e.g., Jillett 1969; Heath 1971a, 1971b, 1985; Stanton 1971, 1976; Bradford 1983; Hawke 1989). However, the combination of these data with near real-time SST imagery and with fluorescence, particulate, and nutrient profiling provides a unique overview of the biological environments which characterise the coastal and offshore waters of the South Island.

The T-S characteristics plotted in Fig. 3 derive in part from the zonal position of New Zealand waters in the South Pacific Ocean, and in part from a broad range of local influences, particularly in the surface mixed layer. Almost all of the deeper waters followed the same linear T-S relationship. This tight relationship represents the mixing curve between Subtropical Lower Water (STLW) and Antarctic Intermediate Water (AAIW) (B. R. Stanton, New Zealand Oceanographic Institute, unpubl. data). The high salinity of STLW results from evaporation at the

centre of the subtropical gyre to the north of New Zealand. This water then flows southwards and is diluted near the surface by the freshwater influenced shelf water, resulting in a subsurface salinity maximum recorded previously off the west coast between 11 m and 250 m (Stanton unpubl. data). Subsurface salinity maxima were commonly observed during the present cruise, for example at 100 m depth off Doubtful Sound, and at 50 m in Karamea Bight. These features were sometimes accompanied by a temperature maximum at the same depth, further reflecting the subtropical origins of this water. AAIW has a salinity minimum of about 34.44 psu, but off the west coast this minimum occurs at about 1000 m (Stanton 1971), well below the maximum depth of sampling in the present study. The tongue of subsurface high-salinity water on the east coast transect extended at least 150 km to the south of Chatham Rise (Fig. 14). This tongue can extend c. 1400 km to the Polar Front in other regions, but its southward extent is limited by the Chatham Rise in this area (Heath 1976).

The T-S curve for Cook Strait Station R387 (Fig. 3) deviated substantially from the other deep profiles. Three separate currents come together in southern Cook Strait (Fig. 1B): the D'Urville Current which brings in subtropical water eastwards and southwards from the west coast of the North Island, the East Cape current which delivers water flowing southwards along the east coast of the North Island, and the Southland current which flows northwards along the east coast of the South Island (Heath 1985). This is a region of mixing and complex hydrodynamic exchange, and the unusual T-S plot is probably a reflection of these disparate origins.

The sharply defined front in Cook Strait observed in the SST images (Fig. 2 and 4) appears to be a variable feature that is formed by the incursion of the warm D'Urville Current down the western side of the North Island (the Manawatu Coast) into cool, tidally mixed Southland Current and upwelled water in southern Cook Strait (Bowman et al. 1983; Bradford et al. 1986). This incursion is probably driven by northerly winds (Bowman et al. 1983), and the strength and position of the thermal front is therefore likely to be highly dependent on recent weather conditions. Unfortunately, no concurrent data are available from south of the front, but the profiling at Station R387 revealed a complex vertical structure in all biological and environmental variables that was not apparent from the surface properties.

The inshore band of cold water extending down the west coast of the South Island and the upward

tilting of nutrient, temperature, and salinity isopleths (Fig. 9) are consistent with upwelling as described for this region by Stanton (1971, 1976). The low inshore temperatures are unlikely to be the direct effect of cold riverine inflows because these inputs are substantially diluted by mixing with the sea close to the coast and the difference between river and sea temperatures is not large. In hydrographic surveys around the Buller and Karamea River mouths, for example, there is a well-defined effect on the salinity field, but it is rarely associated with a major temperature anomaly (Stanton 1972). It is possible, however, that the freshwater inflow contributes to the cooler surface temperatures indirectly by producing a shallower mixed layer that because of its reduced volume is subject to more rapid cooling by heat exchange with the atmosphere (in winter) and by the input of cold upwelled water. Small patches of the coldest water in our West Coast SST images (e.g., 12–13°C, blue, Fig. 6) occurred in the immediate vicinity of the mouths of the largest rivers along the coast. The mean discharges for May 1989 were (see Fig. 1): Buller River, 178 m³ s⁻¹; Grey River, 219 m³ s⁻¹; and Whataroa River (discharging at Abut Head), 74 m³ s⁻¹ (Water Resources Survey unpubl. data).

Figures 2, 4, and 6 emphasise the highly irregular distribution of cool inshore temperatures that may derive from upwelling along the South Island west coast. The plumes which extended up to 75 km seawards resemble the seaward jets or "squirts" reported in other upwelling environments where they are an important mechanism of cross-shelf transport (e.g., Kosro & Huyer 1986). These features appear to be highly transient in the west coast setting, and frequently associated with specific topographic features (M. Moore, New Zealand Oceanographic Institute, unpubl. data). The sampling of the plumes north of the Buller River and off Abut Head show that they are composed of a relatively shallow layer of low salinity water with considerable variability from site to site and with depth in their nutrient and biological particulate characteristics. The most extensive area of cold water occurred in the plume that extended northwards from Cape Foulwind, its orientation probably dictated by the Westland Current and its size dictated by the huge discharge of the Buller River on this coastline. The shallow mixed layer which accompanies these extensive offshore plumes is likely to exert a major influence on the biological environment. A modelling analysis of microbial food chain processes for this region has shown that the conditions which result from the

combination of upwelling and mixed-layer shoaling could lead to enhanced growth rates of all components of the inshore plankton (Kumar et al. in press).

The waters south of the South Island (Tables 2 and 3) contain regions of strong gradients and mixing between the cool subantarctic water and warmer, more saline subtropical water. The most saline (34.82 psu) and warmest (12.98°C) conditions in Foveaux Strait were in the west indicating the intrusion of subtropical water via the current which sweeps around the south-west South Island and ultimately becomes the Southland Current (Fig. 1B). The satellite imagery (Fig. 2 and 10) is consistent with these observations, showing a tongue of warmer water (13–14°C; yellow in Fig. 2, red in Fig. 10) penetrating into Foveaux Strait from the west. The elevated nutrient concentrations relative to offshore waters along the west coast, however, imply some mixing with subantarctic water as far west as Station R401.

The fluorescence, temperature, and salinity profiles in Foveaux Strait indicate that these shallow waters are reasonably well mixed vertically. Ammonium and urea remained at or below our limits of detection at most stations and depths throughout the cruise, but in Foveaux Strait there was a measurable increase in these highly labile nitrogen substrates towards the sediments. These bottom gradients imply fast rates of reduced nitrogen release by secondary production in the sediments relative to rates of diffusion and advection in the overlying water column.

The SST images in the Chatham Rise region show a surface tongue of cool water penetrating northwards through Mernoo Gap. This temperature feature is consistent with the upwelling of deep Southland current water moving northwards and rising up over the saddle (Heath 1981) although it may simply represent the northward advection of cold Southland Front water at the surface. Reactive phosphorus concentrations up to 0.95 mmol m⁻³ have been previously recorded here, highly suggestive of upwelling (Bradford & Roberts 1978).

The large circular feature located at 42°S, 176°E (Fig. 2 and 13) frequently appears on SST images and appears to be more or less permanently stationed off the south-east corner of the North Island (Barnes 1985). It is an anticyclonic eddy (anticlockwise rotation) believed to be formed by the interaction between the East Cape and Southland Currents (Barnes 1985). In our transect over Chatham Rise we identified another eddy-like feature positioned over

Mernoo Bank. In the CTD sections it appears as a thermostad region of homogeneous warm temperature and high salinity indicative of its subtropical origin. The mixed layer was much deeper than water to the north and south, with elevated nitrate concentrations and reduced chlorophyll *a* levels. These features may reflect the short residence time of phytoplankton within the patch and/or the light-limitation of their growth rates relative to the shallower mixed-layer environment in the ocean to the north and south.

The correlation analysis reported here showed that there was little relationship between the biological particulates and the physical or chemical variables in either the overall data set (Table 6) or the Chatham Rise subset (Table 7). This is consistent with observations by Viner & Wilkinson (1988) in the Western Cook Strait region where there was also no correspondence between chlorophyll *a* and nitrate. The concentration of phytoplankton biomass at any one location results from a complex balance between production and loss processes, and it is not unexpected that there is little correlation with specific environmental state variables. However, nutrient concentrations correlated well with the zonal variations in temperature (Tables 6 and 7) and salinity (Table 7). These data were obtained in autumn when light was potentially a limiting factor for algal growth, and this zonal relationship may be less apparent at other times when (or if) much higher phytoplankton biomass and nutrient depletion is achieved. Both NO_3 and DRP decreased in the subtropical water, but NO_3 to a greater extent, giving a strong inverse correlation between nutrient N:P ratios and temperature (Tables 6 and 7). This implies an increasing shift towards N limitation at lower latitudes.

In vivo fluorescence profiling is an oceanographic technique of widespread use internationally, but has only recently been applied to the seas around New Zealand. In the present study the profiles provided an immediate and informative guide to the lower depth limit of the phytoplankton and gave a detailed picture of the vertical changes in biomass in relation to physical and chemical gradients down the water column. This record was obtained in real time on board the ship and could therefore be used to select the appropriate depths for discrete nutrient and particulate sampling. Several of the profiles showed a series of pronounced fluorescence discontinuities associated with sharp gradients in temperature and/or salinity (e.g., Stations R388, R400). The cause of such variations remains unknown but the profiles

suggest abrupt shifts in phytoplankton community structure or physiology between adjacent strata.

Although fluorescence correlated well with extracted chlorophyll *a* down each profile, the exact relationship between the two variables changed substantially between stations, and in the overall data set chlorophyll *a* explained only 58% of the variance in fluorescence. This is consistent with the well-known influences of a broad range of biological factors on fluorescence yield ($F_{\text{Chl. } a}$) including cell size (Alpine & Cloern 1985), taxonomic composition (Vincent 1984), and photophysiological processes (Vincent in press).

The large variations in $F_{\text{Chl. } a}$ across the Chatham Rise and its significant correlation with such a large number of other variables indicates a systematic effect of the environment on this ratio, but does not allow the primary causal factors to be identified. It is possible, for example, that higher chlorophyll *a* concentrations (and depleted nutrients) are accompanied by a shift towards larger-celled phytoplankton; this would account for the reduced $F_{\text{Chl. } a}$ (e.g., Alpine & Cloern 1985), its significant inverse relationship with chlorophyll *a* concentration, and positive relationship with nutrients.

The SST imagery obtained during this cruise provided a useful overview of the distribution of water masses around New Zealand, and given the correlation between temperature and NO_3 , DRP, Si, and N:P ratios, provided a first order guide to the nutritional environment for the phytoplankton. Without vertical sea truth information, however, the application of satellite images of sea surface temperature as a guide to the planktonic environment, surface colour as a measure of phytoplankton biomass, or surface fluorescence as a measure of productivity, will be severely limited in New Zealand waters. Our analyses show that the depth of the mixed layer containing the phytoplankton varies enormously with location, and features such as the west coast plumes and the eddy-like patches near the Chatham Rise are associated with large perturbations of the upper water column that are likely to influence strongly the vertical structure and productivity of the plankton. Surface chlorophyll *a* concentration was an imprecise index to the total water column standing stock of chlorophyll in the overall data set ($r^2 = 0.42$) but the much better fit in the Chatham Rise subset ($r^2 = 0.88$) suggests that specific locations can be identified within the New Zealand Exclusive Economic Zone where satellite imagery of sea surface properties will provide a reliable biological index.

ACKNOWLEDGMENTS

We thank Liana Hrstich and Stu Pickmere for technical assistance; Janet Bradford, Mike Moore, Ken Grange, Basil Stanton, and Ron Heath for helpful advice and discussion throughout all stages of this work; Julie Hall, Anthony Cole, Lynell May, Stu Pickmere, and Rob Davies-Colley for shipboard assistance; the master and crew of Cruise 2027 of RV *Rapuhia*; Janet Simmiss for word-processing support; and Tangaroa for such a remarkable number of cloud-free satellite passes during the cruise.

REFERENCES

- Alpine, A. E.; Cloern, J. E. 1985: Differences in in vivo fluorescence yield between three phytoplankton size classes. *Journal of plankton research* 7: 381–390.
- Barnes, E. J. 1985: Eastern Cook Strait region circulation inferred from satellite-derived sea-surface temperature data. *New Zealand journal of marine and freshwater research* 19: 405–411.
- Bowman, M. J.; Kibblewhite, A. C.; Chiswell, S. M.; Murtagh, R. A. 1983: Shelf fronts and tidal stirring in greater Cook Strait, New Zealand. *Oceanologica acta* 6: 119–129.
- Bradford, J. M. 1983: Physical and chemical oceanography of the west coast of South Island, New Zealand. *New Zealand journal of marine and freshwater research* 17: 71–81.
- Bradford, J. M.; Roberts, P. E. 1978: Distribution of reactive phosphorus and plankton in relation to upwelling and surface circulation around New Zealand. *New Zealand journal of marine and freshwater research* 12: 1–15.
- Bradford, J. M.; Lappenas, P. P.; Murtagh, R. A.; Chang, F. H.; Wilkinson, V. 1986: Factors controlling summer phytoplankton production in greater Cook Strait, New Zealand. *New Zealand journal of marine and freshwater research* 20: 253–279.
- Hawke, D. J. 1989: Hydrology and near-surface nutrient distribution along the South Otago continental shelf, New Zealand, in summer and winter 1986. *New Zealand journal of marine and freshwater research* 23: 411–420.
- Heath, R. A. 1971a: The Southland Current. *New Zealand journal of marine and freshwater research* 6: 497–533.
- 1971b: Hydrology and circulation in central and southern Cook Strait, New Zealand. *New Zealand journal of marine and freshwater research* 5: 178–199.
- 1976: Models of the diffusive-advective balance at the subtropical convergence. *Deep-sea research* 23: 1153–1164.
- 1981: Physical oceanography of the waters over the Chatham Rise. *New Zealand Oceanographic Institute summary* 18: 1–15.
- 1985: A review of the physical oceanography of the seas around New Zealand—1982. *New Zealand journal of marine and freshwater research* 19: 79–124.
- Heath, R. A.; Ridgway, N. M. 1985: Variability of oceanic temperature and salinity fields on the West Coast continental shelf South Island, New Zealand. *New Zealand journal of marine and freshwater research* 19: 233–245.
- Heath, R. A.; Gilmour, A. E. 1987: Flow and hydrological variability in the Kahurangi Plume off north-west South Island, New Zealand. *New Zealand journal of marine and freshwater research* 21: 125–140.
- Jillett, J. B. 1969: Seasonal hydrology of waters off the Otago Peninsula, southeastern New Zealand. *New Zealand journal of marine and freshwater research* 3: 349–375.
- Kosro, P. M.; Huyer, A. 1986: CTD and velocity surveys of seaward jets off Northern California, July 1981 and 1982. *Journal of geophysical research* 91: 7680–7690.
- Kumar, S. K.; Vincent, W. F.; Austin, P. C.; Wake, G. D. in press: Picoplankton and marine food chain dynamics in a variable mixed layer: a reaction diffusion model. *Ecological modelling*.
- McMillin, L. M.; Crosby, D. S. 1984: Theory and validation of the multiple window sea surface temperature technique. *Journal of physical research* 89: 3655–3661.
- Nilsson, C. S.; Tildesley, P. C. 1986: Navigation and remapping of AVHRR imagery. In: Prata, A. J. ed. First Australian AVHRR Conference, Perth, Western Australia, 22–24 Oct. 1986. Perth, CSIRO Division of Groundwater Research.
- Stanton, B. R. 1971: Hydrology of Karamea Bight, New Zealand. *New Zealand journal of marine and freshwater research* 5: 141–163.
- 1972: Two-dimensional model of diffusion processes around a river mouth. *New Zealand journal of marine and freshwater research* 6: 329–342.
- 1976: Circulation and hydrology off the west coast of the South Island, New Zealand. *New Zealand journal of marine and freshwater research* 10: 445–467.
- Stanton, B. R.; Ridgway, N. M. 1988: An oceanographic survey of the subtropical convergence zone in the Tasman Sea. *New Zealand journal of marine and freshwater research* 22: 583–593.
- Strickland, J. D.H.; Parsons, T. R. 1972: A practical handbook of seawater analysis (2nd edition). *Bulletin* 167, Fisheries Research Board of Canada.
- Vincent, W. F. 1984: Fluorescence properties of the freshwater phytoplankton: three algal classes compared. *British phycological journal* 18: 5–21.

- in press: The dynamic coupling between photosynthesis and light in the phytoplankton environment. *Verhandlungen, Internationale Vereinigung für theoretische und angewandte Limnologie*.
- Vincent, W. F.; Chang, F. H.; Cole, A.; Downes, M. T.; James, M. R.; May, L.; Moore, M.; Woods, P. H. 1989: Short-term changes in planktonic community structure and nitrogen transfers in a coastal upwelling system. *Estuarine coastal and shelf science* 29: 131–150.
- Viner, A. B.; Wilkinson, V. H. 1988: Uptake of nitrate and ammonium, and distribution of related variables in the upwelling plume of western Cook Strait/Taranaki Bight. *New Zealand journal of marine*